Dynamic Structure Factor of Diblock Copolymer Solutions in the Disordered State. 2. Effect of Composition Polydispersity

P. Holmqvist,[†] S. Pispas,[‡] R. Sigel,[†,§] N. Hadjichristidis,*[,‡] and G. Fytas*[,†]

FORTH−Institute of Electronic Structure and Laser, P.O. Box 1527, 711 10 Heraklion, Crete, Greece, and Department of Chemistry, University of Athens, 15701 Zografou, Athens, Greece

Received November 1, 2001; Revised Manuscript Received January 14, 2002

ABSTRACT: The dynamic structure factor of entangled solutions of one symmetric and two asymmetric high molar mass styrene-*b*-ethylene-*alt*-propylene (SEP) and the parent styrene-*b*-isoprene (SI) diblock copolymers in the common solvent toluene was thoroughly studied by photon correlation spectroscopy. The incomplete hydrogenation transforms the I-block of SI into a random heteropolymer block. In turns out that this acts as enhanced composition polydispersity on both static and dynamic structure factor. In the mean-field regime of the disordered phase, the decay of the composition fluctuations in SI and SEP changes from a pure relaxational (q-independent rate) for SI to a pure diffusive (q^2-dependent rate) character for SEP in a controlled way.

Introduction

The prediction of the dynamic response of diblock copolymers relies on the identification of the dominant mechanisms in the relaxation of the order parameter (composition) fluctuations, $\phi_q(t)$, manifested in the intermediate scattering function (dynamic structure factor) $S(q,t)$ of the system. The most probable ϕ_q have a wave vector $q \sim q^*$ with $q^*R \sim O(1)$ (R being the radius of gyration), and hence the static structure factor $S(q)$ peaks[1] at a finite q^*. In the mean-field regime, the $S(q \leq q^*,t)$ of disordered diblock copolymers[2,3] is a two-step decay function assigned to overall chain relaxation with characteristic rate $\Gamma_1 \sim 1/\tau_1$ (τ_1 is the longest relaxation time) and chain self-diffusion with $\Gamma_2 = D_s q^2$ (D_s is the self-diffusion coefficient). On the contrary, the $S(q,t)$ of symmetric styrene−isoprene (SI) diblocks assumes a single decay with a purely diffusive rate.[4] The domination of the slow diffusive mode in $S(q,t)$ was attributed to the presence of polydispersity in both molecular mass and composition of the real diblock copolymers. For a better understanding of the shape of $S(q,t)$ in the mean-field regime, the reported difference in the dynamic response of the symmetric[3] and asymmetric[2] high molar mass SI should be unambiguously clarified.

A controlled increase of composition polydispersity $\kappa_0 = \langle f^2 \rangle - \langle f \rangle^2$ in diblock copolymers would require a rather tedious procedure involving the synthesis of monodisperse samples with different average composition f and the same molar mass M_w and subsequent on appropriate mixing. Instead, the hydrogenation of the PI block in a SI diblock conveniently produces a twin S-*b*-(I-r-ethylene-*alt*-propylene) (SEP) with composition heterogeneity depending on the overall conversion and the composition of the parent SI. In this chemical transformation of SI into SEP, M_w and M_w/M_n are preserved as easily proved by light scattering measurements and GPC. However, the change in the chemical nature modifies the interaction parameter χ and the optical contrast that should be considered prior to the experimental performance. SEP is less compatible as suggested by the observation that the SEP/toluene solutions microphase separate at lower concentrations than their parent SI/toluene solutions (Table 1). The disparity in χ between SI and SEP should cause unequal contributions of the diffusive process,[5]

$$S_2 = \kappa_0/(1 - 2\chi\kappa_0\phi^{1.6}N), \quad \Gamma_2 = q^2 D_s(1 - 2\chi\kappa_0\phi^{1.6}N) \tag{1}$$

in $S(q,t)$ where N is the total number of monomers in the chain. The restriction to low polymer volume fractions, ϕ, well within the disordered regime suppresses differences of this origin as can readily be checked by contrasting Γ_2/q^2 with D_s. In this disordered regime, mismatch in the interactions between PI and PEP segments can also be neglected as being sufficiently diluted. The difference in the optical contrast (refractive index) between the blocks in SI and SEP amounts up to about twice higher intensity I_2 ($\propto NS_2$) for SEP.

Since the consequence of the above chemical alterations can be controlled, a modified behavior in the dynamic structure factor of SEP can formally arise from enhanced composition heterogeneities in SEP chains due to their different content in PEP. Thus, the relative contribution of the two relaxation mechanisms (chain overall motion and diffusion) to the $\phi_q(t)$ with wavelength $2\pi/q$ can be examined.

In this report, we show that the introduction of a different degree of composition polydispersity in well-fractionated asymmetric and symmetric SI block copolymers by partial hydrogenation (∼75%) to S-*b*-(I-r-ethylene-*alt*-propylene) (SEP) alters the mean-field behavior of $S(q,t)$ expected for monodisperse diblock copolymers[6] in the vicinity of q^*. Hence, irrespective of the average diblock composition, disordered diblock copolymers in the mean-field regime display a predicted dynamic response.

Experimental Section

Polymer Synthesis. The high molecular weight SI diblocks were synthesized by anionic polymerization techniques as described elsewhere.[2] Because of the low concentration for the living ends, some deactivation of the PS block occurred by the

[†] FORTH−Institute of Electronic Structure and Laser.
[‡] University of Athens.
[§] Present address: Max Planck Institute of Colloids and Interfaces, 14476 Golm, Germany.

10.1021/ma0119068 CCC: $22.00
Published on Web 04/02/2002

Table 1. Sample Characteristics of High Molecular Mass Styrene-*b*-isoprene (SI) and Styrene-*b*-ethylpropylene (SEP)[a] Diblocks

sample	$M_w \times 10^{-6}$ (LALLS)[b]	$M_{w,PS} \times 10^{-6}$ (LALLS)[b]	wt %, PS (NMR)[c]	M_w/M_n (SEC)[d]	c_{ODT} (wt %)[e]	q^* (nm^{-1})[e]
SI2M80	1.60	1.34	85	1.15	9.2	0.0282
(SEP 80)					7.0	0.0249
SI50	0.95	0.49	52	1.06	8.8	>0.035
(SEP 50)					5.4	0.035
SI2M20	1.93	0.49	26	1.09	7.4	0.0306
(SEP 20)					5.0	0.0154

[a] ~75% conversion. [b] THF at 25 °C. [c] $CDCl_3$ at 30 °C. [d] THF at 40 °C. [e] In toluene at 20 °C.

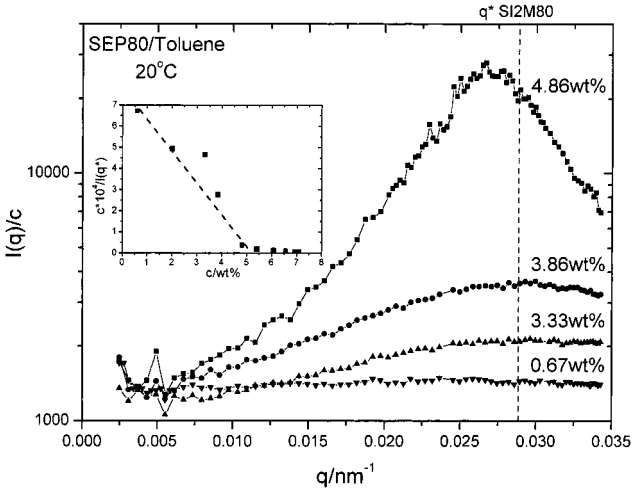

Figure 1. Light scattering intensity distribution $I(q)/c$ for disordered solutions of SEP80 in toluene at four different concentrations c at 20 °C. The vertical line indicates the peak position q^* for the precursor SI2M80 (ref 3). Inset: $c/I(q^*)$ vs c.

addition of isoprene. Five solvent /nonsolvent (toluene/methanol) fractionations were employed for the isolation of pure diblocks. The molecular characteristics of the two asymmetric[2] and one symmetric SI samples are given in Table 1. The SEP samples are obtained by hydrogenating the PI block using the Wilkinson catalyst in toluene under hydrogen pressure.[7] The extent of hydrogenation amounts to ca. 75% for all samples as determined by ^{1}H NMR spectroscopy.[8]

Photon Correlation Spectroscopy (PCS). The intermediate scattering function $C(q,t) = [G(q,t) - 1)/f^*]^{1/2}$ is obtained from the experimental intensity autocorrelation function $G(q,t)$ (f^* is the instrumental coherence factor) measured by PCS in the polarized geometry under homodyne conditions over a broad time range (10^{-7}–10^2 s) at a scattering wave vector $q = (4\pi n/\lambda) \sin(\theta/2)$ (λ is the laser wavelength in a vacuum, n is the refractive index, and θ is the scattering angle) ranging from 3×10^{-3} to 3.5×10^{-2} nm^{-1}. An ALV-5000 full digital correlator was employed in conjunction with a Nd:YAG laser at $\lambda = 532$ nm. All measurements were carried out at 20 °C.

The characteristic diblock copolymer peak in the scattering intensity $I(q)$ falls within the light scattering q's as shown in Figure 1 for solutions of SEP80 in toluene at $c < c_{ODT}$, where c_{ODT} (Table 1) is the concentration at which the semidilute solution undergoes the disorder-to-order transition at 20 °C and $I(q)$ are normalized intensities by the polarized intensity of the neat toluene. The maximum of $I(q^*)/c$ at q^* increases strongly with c beyond about 4 wt % which signifies the onset of strong composition fluctuations approaching the ODT; c_{ODT} exceeds its mean-field value obtained from the linear extrapolation of $c/I(q^*)$ in the inset of Figure 1. Since in the present investigation the subject of interest is the disordered phase in the mean-field regime, all solutions of samples of Table 1 fall within this regime.

Results and Discussion

Asymmetric Diblock Copolymers. The intermediate scattering function $C(q,t)$ ($\propto S(q,t)$) for 3.3 wt % SEP80 solution at $q = 9.1 \times 10^{-3}$ nm^{-1} is shown in Figure 2. The representation[2] of $C(q,t)$ proceeds via inverse Laplace transformation (ILT)

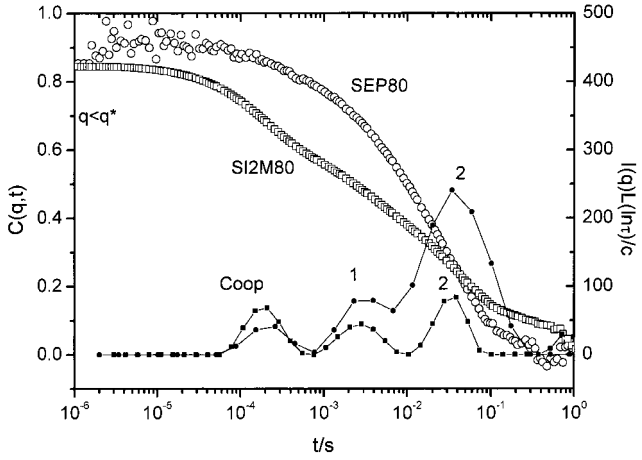

Figure 2. Intermediate scattering functions $C(q,t)$ at $q = 9.1 \times 10^{-3}$ nm^{-1} for 3.3 wt % SEP80 (○) and 3.9 wt % SI2M80 (□, ref 2) in toluene at 20 °C along with the distribution of relaxation times $I(q)L(\ln \tau)/c$ (eq 2)(solid symbols). The peaks in $L(\ln \tau)$ associated with the cooperative diffusion and the relaxation (1, 2) of the composition fluctuations are indicated in the plot.

$$C(q,t) = \int L(\ln \tau) \exp(-t/\tau)\, d(\ln \tau) \qquad (2)$$

where the distribution of relaxation times $L(\ln \tau)$ is also included in Figure 2. The nonexponential shape of $C(q,t)$ is clearly revealed by its ILT, leading to the non single distribution relaxation function $L(\ln \tau)$. The position and the area of each peak in $L(\ln \tau)$ define the rate, Γ_i, and intensity, I_i, of the particular process. Three relaxation processes were found to be the optimum solution of eq 2 based not only on the fit quality but also on the consistent and physically meaningful results (see below). In this context, SEP80 and SI2M80 (ref 2) (included in Figure 2 for comparison) qualitatively behave alike. The first peak at short times related to the cooperative diffusion,[9] responsible for the relaxation of the total diblock concentration fluctuations, is not diblock copolymer specific. The other two processes relate to the composition fluctuations $\phi_q(t)$ and are identified with the chain relaxation and chain self-diffusion process in the mean-field regime. In this case, $C(q,t)$ can be described by

$$C(q,t) = a_1(q) \exp(-\Gamma_1 t) + a_2(q) \exp(-D_s q^2 t) \qquad (3)$$

where the static structure factor $S_1(q) \propto I_1(q)/c = a_1(q)I(q)/c$ attains its maximum at q^*. The second dynamic contribution in eq 3 is due to the presence of composition polydispersity κ_0 in real diblocks, and the

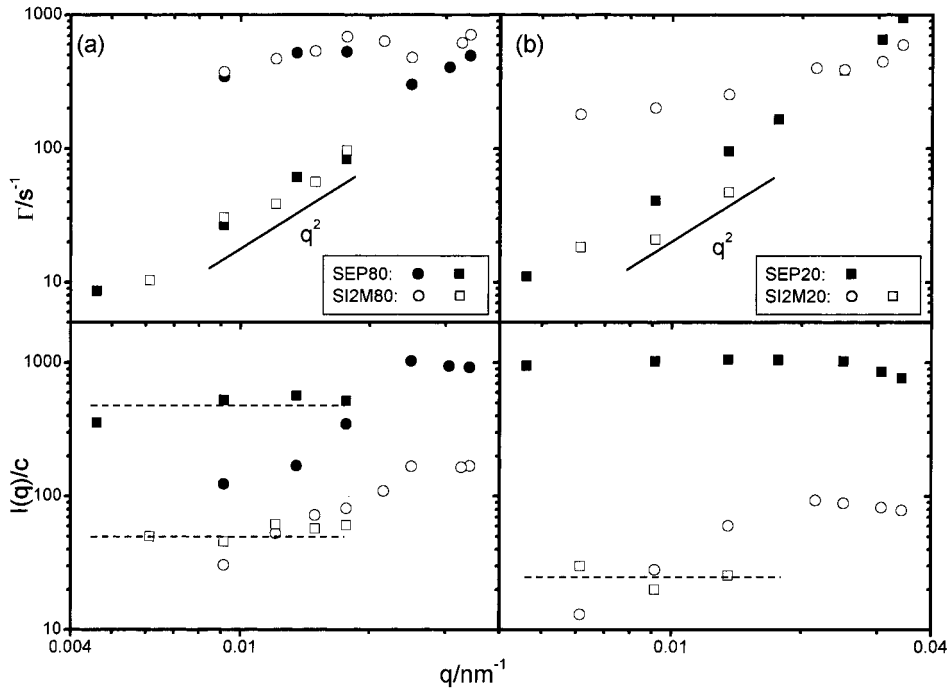

Figure 3. Relaxation rates Γ_i and intensities I_i/c ($i = 1, 2$) associated with the two relaxation processes of the dynamic structure factor at different wave vectors q in (a) SEP80 (3.3 wt %), SI2M80 (3.9 wt %) and (b) SEP20 (2.0 wt %), SI2M20 (2.2 wt %). Circles and squares are for chain relaxation ($i = 1$) and self-diffusion ($i = 2$), respectively. Solid line indicates diffusive behavior.

associated incoherent scattering intensity $S_2 \propto \alpha_2(q)$-$I(q)/c$ is proportional to κ_0. In a static scattering SAXS or SANS experiment the measured quantity is the sum of $S_1(q)$ and S_2. The design of the present systems allows for a serious check of the shape of $C(q,t)$.

Quantitatively, the relative contributions of the two processes of eq 3 to the $C(q,t)$ of SEP80 and SI2M80 are different. Figure 3a shows that the intensity $I_2(q)/c \propto S_2$ of SEP80 exceeds that of SI2M80 more than expected from the optical contrast. On the other hand, the intensity $I_1(q)/c$ for the two samples scales with the optical contrast in the q range where the two processes are resolved. Apparently, the higher composition heterogeneity κ_0 in SEP80 enhances the intensity I_2 (eq 1) of the diffusive process in $S(q,t)$. Taking into account the difference in the optical contrast, the I_2/c data in Figure 3a suggest that S_2 is about 4 times stronger in SEP80. This disparity in κ_0 might explain[10] the shift of the peak position q^* of the $S(q)$ for SEP80 below the q^* for SI2M80 (Table 1 and Figure 1); otherwise, the similar size of this pair would not allow for different q^*. Concerning the dynamics both Γ_1 and $\Gamma_2(q)$ assume very similar values in the two systems consisting of chains with the same N. In view of eq 1, the similarity of the $\Gamma_2(q)$ values implies a negligible effect of χ, and therefore $\Gamma_2(q)/q^2$ should be the self-diffusion coefficient. In fact, D_s from PFG-NMR measurements compare well with the $\Gamma_2(q)/q^2$ of the PCS experiment (see Figure 5).

The PI block in SI2M80 is short compared to the PS block (Table 1), and hence the hydrogenation produces moderate composition heterogeneities in SEP80; the bimodal shape of eq 3 holds for SEP80 as well. A significant stronger disturbance in the composition homogeneity should then be expected by hydrogenating SI2M20. The comparison between the $C(q,t)$ of SEP20 and SI2M20 and the underlying distribution, $L(\ln \tau)$, at the same q are depicted in Figure 4. One process mainly dominates the relaxation of $\phi_q(t)$ in SEP20 in contrast to the well-resolved two processes in SI2M20

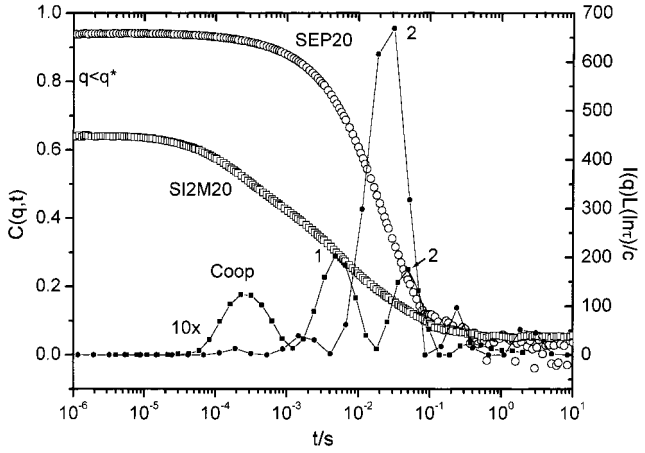

Figure 4. Intermediate scattering functions $C(q,t)$ at $q = 9.1 \times 10^{-3}$ nm^{-1} for 2.0 wt % SEP20 and 2.2% SI2M20 in toluene at 20 °C along with the normalized distribution of relaxation times $I(q)L(\ln \tau)/c$ (eq 2) (solid symbols). For SI2M20 the latter is multiplied by a factor of 10 while the peak labels are as in Figure 2.

according to eq 3. The intensity of the main process in SEP20 is about 40 times higher than the intensity I_2/c in SI2M20. The q dependence of the intensities $I_i(q)/c$ and the rates $\Gamma_i(q)$ associated with the relaxation modes of Figure 4 is shown in Figure 3b. The single process in SEP20 exhibits a pure diffusive rate that compares well with the self-diffusion rate in SI2M20 (ref 2). However, the intensity largely exceeds that of the SI2M20 apparently due to the much larger composition heterogeneity in SEP20. The fast relaxation process (first decay in eq 3) in SI2M20 cannot be resolved in SEP20.

Thus, the $C(q,t)$ of SEP20 assumes diffusive behavior dominated by the second decay of eq 3, in contrast to the behavior of its precursor SI2M20. This pertinent finding is unique since it is supported by the q dependence of both the rates and intensities shown in Figure

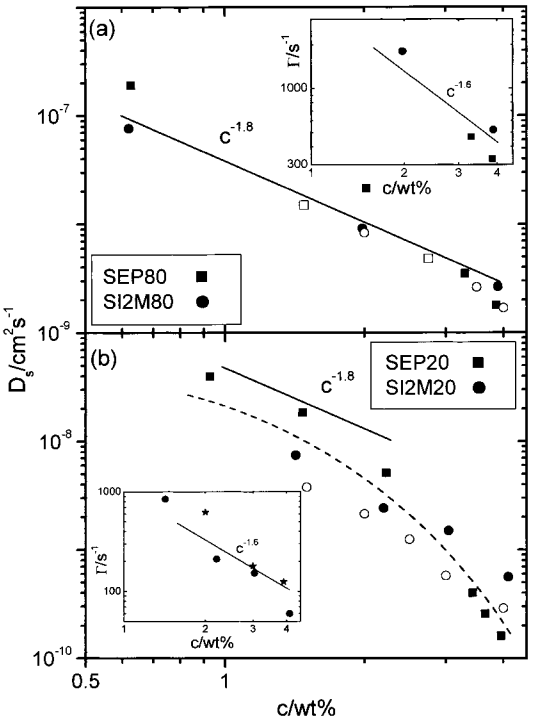

Figure 5. Chain self-diffusion coefficient (D_s) and relaxation rate (Γ_1) as a function of diblock concentration c: (a) SEP80 (□) and SI2M80 (○) inset: Γ_1 for both systems; (b) SEP20 (□) and SI2M20 (○), inset: Γ_1 for SI2M20 (from PCS (●) and rheology (*). Solid and open symbols in (a) and (b) indicate D_s from PCS and PFG-NMR (ref 14 for SI2M20 and SI2M80). Scaling predictions for semidilute entangled polymer solutions are indicated in the plot.

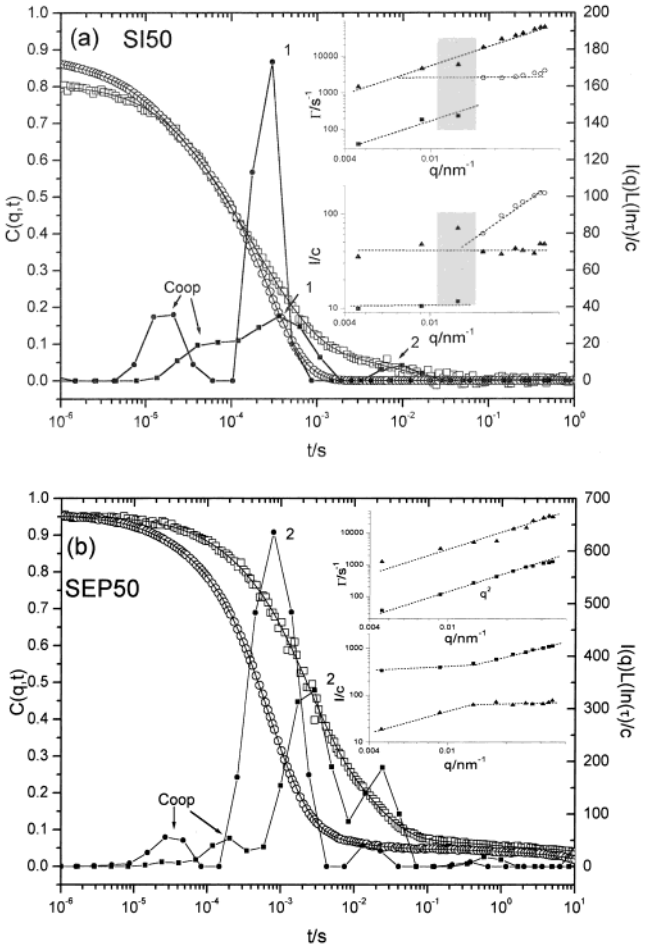

Figure 6. Intermediate scattering function and the distribution of relaxation times, $I(q)(L(\ln \tau)/c$ (solid symbols), at two wave vectors q (□, 0.0177 nm^{-1}; ○, 0.035 nm^{-1}) and 20 °C for 2.85 wt % SI50 (a) and 2.88 wt % SEP50 (b) toluene solutions. The relaxation rate Γ_i and the associated reduced intensity I_i/c of the resolved processes (i = 1, 2, 3) are shown as a function of q in the insets (cooperative diffusion (▲), chain overall motion (○), and self-diffusion (■)). In the shaded regions (in the inset of a) the proximity of the two relaxation rates affects the resolution of the two processes. The peaks in $L(\ln \tau)$ associated with the cooperative diffusion and the relaxations (1, 2) of the composition fluctuations are as in Figures 2 and 4.The third peak at long times in the $L(\ln \tau)$ of SEP50 (b) does not affect the resolution of the other processes and is probably due to the hydrogenation.

3b. Further support is provided by the concentration dependence of the transport quantities D_s and Γ_1. Moreover, these quantities compare well with the self-diffusion coefficient and the largest relaxation time obtained independently by PFG-NMR and shear rheology, respectively, as shown in Figure 5. Ignoring the concentration dependence of the local friction, the predicted c dependences, in the entangled regime, $D_s \sim c^{-1.8}$ and $\Gamma_1 \sim c^{-1.6}$ approximate the experimental slowing down quite satisfactorily for SEP80 and SI2M80 (Figure 5a). For SEP20, the stronger c dependence of D_s above about 3% is due to the retardation[11,12] of chain motion induced by non-mean-field composition fluctuations approaching the ODT (Table 1).

A theoretical account for the different relaxational behavior of $S(q,t)$ is feasible for symmetric diblocks.[4] Therefore, we consider next the $S(q,t)$ of SI50 and SEP50 disordered solutions.

Symmetric Diblock Copolymers. Figure 6a shows the intermediate scattering function $C(q,t)$ for the 2.85 wt % SI50/toluene solution at two q's (0.0177 and 0.035 nm^{-1}) along with the relaxation time distribution function $L(\ln \tau)$ (eq 2). The main contribution in $C(q,t)$ does not vary with q as reflected in the location of the main peak of $L(\ln \tau)$. This insensitivity of $C(q,t)$ to the q variation resembles that of the asymmetric SI's (ref 2) but clearly contrasts that of the symmetric SI (Figure 2 in ref 4) where the main process was purely diffusive; the $C(q,t)$ of the latter and the present SEP50 look alike. The variation of the rates Γ_i and the reduced intensities (I_i/c) with q that constitutes the fingerprint of the observed relaxation modes is visualized in the two insets of Figure 6a for the resolved processes.[2]

The main contribution to $C(q,t)$ arises from composition fluctuations specific to the diblock architecture, and hence $I_1(q)/c$ increases with q and peaks at q^* ($\geq$0.035 nm^{-1}). The decay rate Γ_1 far from the ordering transition and for $q \leq q^*$ is predicted to be q-independent in monodisperse diblock copolymers[6] (eq 3). At 2.85 wt %, the cooperative diffusion rate approaches $\Gamma_1 \simeq 3 \times 10^3$ s^{-1} at about 0.015 nm^{-1} (Figure 6a), and hence the resolution of these two processes with comparable intensities becomes ambiguous (shaded regions in Figure 6a). The third weaker process of $L(\ln \tau)$ with diffusive rate Γ_2 and q-independent I_2/c is resolved at low q's and is assigned to the copolymer chain self-diffusivity. At 2.85 wt %, the value $I_2/c \sim 10$, being the lowest among the samples of this study (cf. Figure 3), is a sensitive index of the composition polydispersity. Note that the polydispersity in the total molar mass, M_w/M_n, is obtained from gel permeation chromatography (GPC); similar M_w/M_n values do not necessarily imply comparable κ_0 values. The $C(q,t)$ of the symmetric

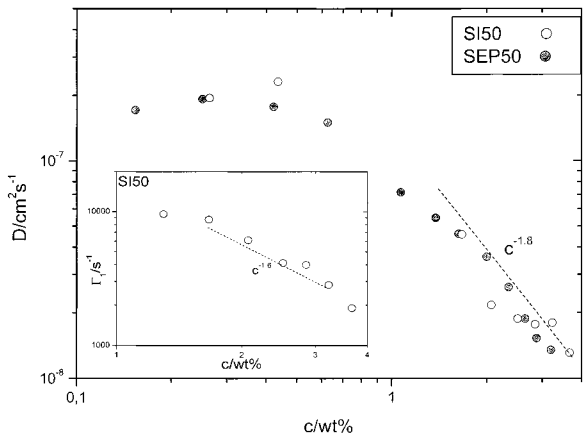

Figure 7. Self-diffusion coefficient of SI50 (open) and SEP50 (solid symbols) as a function of the diblock concentration in toluene at 20 °C. The relaxation rate Γ_1 corresponding to the chain overall motion resolved only in SI50 is shown in the inset. Dashed lines indicate scaling predictions.

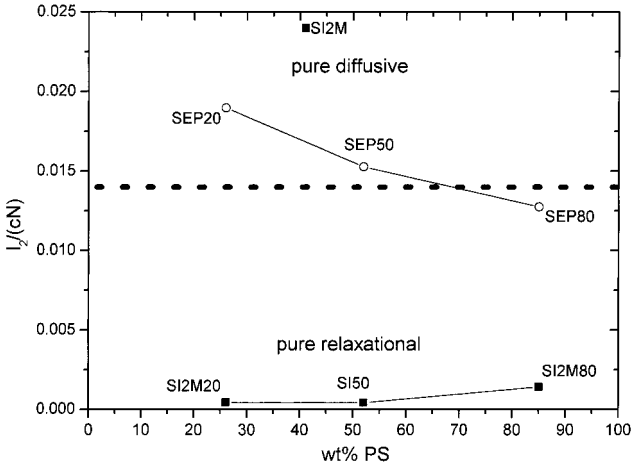

Figure 8. Reduced I_2/cN intensity for the diffusive process of $C(q,t)$ at low q's in SI and SEP (○) as a function of the styrene composition. The $C(q,t)$ becomes pure diffusive for the samples (two SEP and one SI ref 4) falling above the dashed line. The "pure relaxational" characteristic refers to ideal monodisperse diblocks, i.e., $I_2/cN = 0$.

SI2M50 ($M_w/M_n = 1.12$ (ref 4)) was well described only by the diffusive component of eq 3 with relatively high $I_2/c \sim 600$, approaching that of SEP20 (Figure 3b). It appears therefore that in diblocks with such high I_2/c the missing fast mode becomes an inefficient mechanism to relax the $\phi_q(t)$. A trivial explanation might be that the low fraction $I_1(q)/I(q)$ makes the resolution of Γ_1 in the normalized $C(q,t)$ a difficult task. We mention, however, that an enhanced composition polydispersity produced by the addition of polystyrene homopolymer does not affect the resolution of the fast Γ_1 at $q \ll q^*$ for low molar mass diblock copolymers.[13] It might therefore be conceivable that the $\phi_q(t)$ in compositionally heterogeneous disordered diblocks relaxes via collective chain diffusion as for polymer blends.

Figure 6b shows the $C(q,t)$ for a 2.88 wt % SEP50/toluene solution at 20 °C for the two q's of Figure 6a; the relaxation of the concentration fluctuations via cooperative diffusion is very similar in the two samples. The pertinent difference between the $C(q,t)$ in the two samples is the change of the main (structural) relaxation of the composition fluctuations, ϕ_q, from a pure relaxation ($\Gamma \sim q^0$) to a diffusive ($\Gamma \propto q^2$) character. The present situation in SI50 and SEP50 (insets in Figure 6) resembles that of the pair S12M20 and SEP20 in Figure 3b. The intensity I_2 for SEP50 increases with q as for its SI50 parent but assumes a finite value ($I_2/c \approx 300$) at low q's. Also, $I_2(q)$ at the largest $q = 0.035$ nm^{-1} ($q/q^* \approx 1$) is significantly higher in SEP50. Thus, both long ($q \approx 0.14q^*$) and short ($q \approx q^*$) wavelength composition fluctuations are enhanced in SEP50 and decay with a diffusion coefficient $D = \Gamma_2/q^2 = 1.5 \times 10^{-8}$ cm^2/s very similar to the value in SI50 (see Figure 7). The relaxation of ϕ_q via chain overall motion ($\Gamma_1 \approx 2500$ s^{-1}, inset of Figure 6a), the dominant mechanism in SI50, is not resolved in the compositionally polydisperse SEP50. Hence the $S(q,t)$ of SEP50 and SEP20 behave alike. On the basis of the same M_w/M_n of the GPC graphs of SEP and its precursor SI, the very different dynamic behavior between the two pairs of Figures 3b and 6b is unexpected.

The consistency of the data analysis is again supported by the concentration dependence of the resolved dynamics in the two systems as depicted in Figure 7 for the mean-field regime; at 20 °C lamellar microphase occurs at $c_{ODT} \simeq 8.8$ wt % for SI and at 5.4 wt % for SEP/toluene solutions (Table 1). At low concentrations, the translational diffusion in the two systems with the same N expectedly tends to the same limiting value. On the other hand, the agreement at higher concentrations supports the interpretation as chain self-diffusion. In fact, D_s slow down with c conforming to the semidilute entangled scaling[5] $D_s \propto c^{-1.8}$. The overall chain relaxation rate Γ_1 (observed only in SI50) is also a decreasing function of c (inset of Figure 7). Thus, over the considered concentration range, the random PEP block does not affect D_s.

Theoretical Considerations. Figure 8 is a compilation of the intensities associated with the diffusive process in $S(q,t)$ at low q's for all SI and SEP samples. For comparison reasons we plot the reduced I_2/cN taking also into account the different optical contrast between SI and SEP. This map visualizes the boarder between a relaxational to a pure diffusive dynamic response of diblock copolymers. The composition dependence of I_2 in SI and SEP samples indicates a different origin of the composition polydispersity in these samples. In SI, the increasing length of PS with f_s renders the fractionation of SI less effective whereas in SEP it is the increasing length of PI block of the parent SI that enhances composition heterogeneities. The effect of the fractionation on the contributions of the diffusive process to the $S(q,t)$ is indicated by the location of the third SI2M (Table 1, ref 4) sample in the plot of Figure 8. For the latter, the purely diffusive $S(q,t)$ was adequately described by a mean-field theory of the dynamic structure factor of polydisperse symmetric diblocks.[4]

Next, we contrast the experimental dynamic contributions of Figure 6 with the theoretical mean field (without composition fluctuations corrections[1]) $S(q,t)$ of disordered symmetric diblock copolymers with finite polydispersity.[4] Figure 9 visualizes the comparison between theoretical and experimental contributions to the total $S(q,t)$ of disordered diblock copolymers with low (SI50) and high (SEP50) composition polydispersity. The theoretical computation requires the values of R (=50 nm for both samples), Γ_1, composition polydispersity $\langle \delta f^2 \rangle$, proximity to ODT $\epsilon = 1 - (c/c_{ODT})^{1.59}$, and an intensity parameter, A, proportional to the optical contrast between the two blocks.

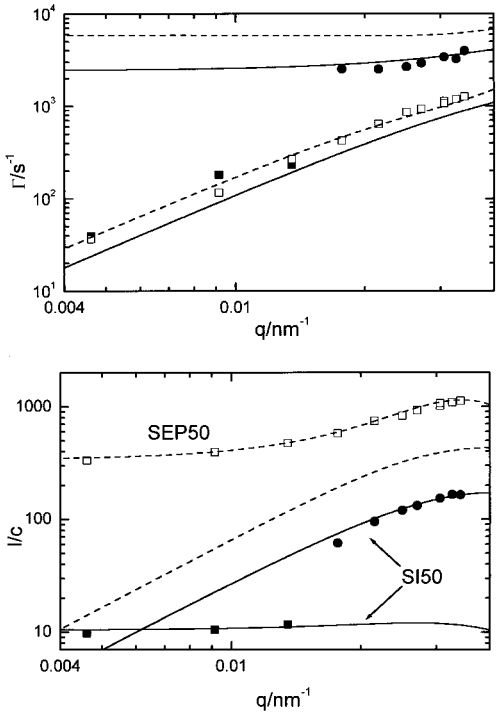

Figure 9. Experimental (points Figure 6a,b insets) and theoretical prediction (lines) for the intensities and relaxation rates of the process(es) associated with the order parameter fluctuations in 2.85 wt % SI50 (solid symbols and lines) and 2.88 wt % SEP50 (open symbols and dashed lines).

In the case of SI50 a good agreement (Figure 9) between theory and experiment for both processes was obtained for $\langle \delta f^2 \rangle = 0.2$ using the experimental values $\Gamma_1 = 2500\ s^{-1}$, $\epsilon = 0.8$, and an adjustable intensity factor A. It is the chain relaxation (I_1, $\Gamma_1 \approx \tau_1^{-1}$) that is the dominant process in SI50 whereas the polydispersity mode (I_2, D_s) is experimentally resolved only at low q's where the intensities I_1 and I_2 become comparable and the rates Γ_1, $D_s q^2$ well separate ($D_s q^2/\Gamma_1 \approx q^2R^2$); note that the experimental $C(q,t)$ is normalized and hence emphasizes the strong process. The relaxation scenario changes in SEP50 in the sense that the dominant process now bears the characteristic of (I_2, Γ_2) in SI50 with about 30 times higher intensity than I_2 in SI at low q's.

We performed the same theoretical representation for SEP50 using fixed Γ_1 (= 2500 s^{-1} as for SI50 because of the same N) and $\epsilon = 0.6$. No successful theoretical description was possible with physical meaningful values of $\langle \delta f^2 \rangle$ and A; $\langle \delta f^2 \rangle$ turns out to be smaller than in SI50, and A is larger than anticipated from the optical contrast. Instead, the theoretical curve for SEP50 in Figure 9 was obtained for $\langle \delta f^2 \rangle = 0.55$, indeed higher than in SI50 (cf. Figure 8), and an intensity factor about twice the A of SI50, but a too low $\epsilon = 0.3$. An adequate mean-field theoretical prediction of both the intensity and the diffusive rate of the single process in SEP50 appears to require closer proximity to ODT ($c_{ODT} \sim 3.7\%$ vs the experimental value of 5.4%) in order to describe well the $I(q \sim q^*)$. It is reasonable to assume that this mean-field theory would reflect an apparent c_{ODT} lower than the actual value (see for example inset to Figure 1). In the case of SI50, the data of Figure 9 correspond to a well disordered state ($c \ll c_{ODT}$) so that the modeling is less sensitive to the value of ϵ.

A shortcoming of the comparison with the theory is the intensity $I_1(q)$ and rate Γ_1 of the fast chain relaxation. The predicted intensity $I_1(q)$ in SEP50 exceeds that in SI50 by a factor of ca. 2, matching the difference in their optical contrast. This suggest that the $I_1(q)$ is not affected by the enhanced composition heterogeneity in SEP50. However, based on the theoretical intensity, $I_1(q)$, and rate, Γ_1, of the missing process in SEP50, we would anticipate the detection of this mode at intermediate q in contrast to the experiment. The theory of $S(q,t)$ of real diblock copolymers is found adequate to describe the experimental single process in the two symmetric SI2M and SI3M of ref 3 and the two processes in the present symmetric SI50. For SEP50, the theory cannot explain the missing chain relaxation mode while it captures the characteristics of the single process through an apparent decrease of c_{ODT}. We should add, however, that in the theory[3] the introduced composition polydispersity preserves the diblock copolymer nature. On the other hand, the heteropolymer nature of the PEP block has negligible contribution to the $I_2(q)/c$ of the SEP. This was checked by examining the excess intensity from semidilute solutions of pure PEP heteropolymer prepared by hydrogenation of a PI ($M_w = 1.2 \times 10^6$) homopolymer.

Concluding Remarks

The dynamic structure factor of disordered symmetric and asymmetric diblock copolymers far from the ODT and q less but near q^* sensitively depends on their composition polydispersity. For monodisperse diblock copolymers, the relaxation of the composition fluctuations with the most probable wavelength ($\sim 1/q^*$) proceeds via chain overall motion whereas for sufficient large composition polydispersity (Figure 8) these fluctuations decay via chain diffusion. The intermediate scattering function $S(q,t)$ was found to vary significantly with the wavelength of the probed composition fluctuations. Thus, the change of $S(q,t)$ from a pure relaxational to a pure diffusive character relates to the degree of the composition polydispersity as reflected in the intensity of the diffusive process at low qR. On the theoretical side, this dynamic crossover behavior can be captured (Figure 9) by a recent mean-field theory of $S(q,t)$ of diblocks with finite composition polydispersity. Whereas the main process in $S(q,t)$ is well represented, the theory probably overestimates the contribution of the fast chain relaxation which can hardly be resolved experimentally.

Acknowledgment. The financial support of the EU (Grant FMRX-CT 97-0112) is gratefully acknowledged. We thank Pr. Ulf Olsson at Physical Chemistry 1 at Lund University for helping us with PFG-NMR measurement and Dr. K. Chrissopoulou for computing the theoretical intermediate scattering function.

References and Notes

(1) Leibler, L. *Macromolecules* **1980**, *13*, 1602. Fredrickson, G. H.; Leibler, L. *Macromolecules* **1989**, *22*, 1238.
(2) Sigel, R.; Pispas, S.; Hadjichristidis, N.; Vlassopoulos, D.; Fytas, G. *Macromolecules* **1999**, *32*, 8447. Semenov, A. N.; Anastasiadis, S. H.; Boudenne, N.; Fytas, G.; Xenidou, M.; Hadjichristidis, N. *Macromolecules* **1997**, *30*, 6280.
(3) Liu, Z.; Pan, C.; Lodge, T. P.; Stepanek, P. *Macromolecules* **1995**, *28*, 3221.
(4) Chrissopoulou, K.; Pryamitsyn, V. A.; Anastasiadis, S. H.; Fytas, G.; Semenov, A. N.; Xenidou, M.; Hadjichristidis, N. *Macromolecules* **2001**, *34*, 2156.
(5) Jian, T.; Anastasiadis, S. H.; Semenov, A. N.; Fytas, G.; Adachi, K.; Kotaka, T. *Macromolecules* **1994**, *27*, 4762.
(6) Erukhimovich, I. Ya.; Semenov, A. N. *Sov. Phys. JETP* **1986**, *28*, 149. Ackasu, A. Z.; Bemmouna, M.; Benoit, H. *Polymer*

1986, *27*, 1935. Bemmouna, M.; Benoit, H.; Borsali, R.; Duval, M. *Macromolecules* **1987**, *20*, 2620.
(7) Mohammadi, N. A.; Rempel, G. L. *J. Mol. Catal.* **1989**, *50*, 259. Hadjichristidis, N.; Iatrou, H.; Pispas, S.; Pitsikalis, M. *J. Polym. Sci., Part A: Polym. Chem.* **2000**, *38*, 3211.
(8) Barth, H. G., Mays, J. W., Eds.; *Modern Methods of Polymer Characterization*; Wiley & Sons: New York, 1991.
(9) De Gennes, P. G. *Scaling Concepts in Polymer Physics*: Cornell University Press: Ithaca, NY, 1979.
(10) Burger, C.; Ruland, W.; Semenov, A. N. *Macromolecules* **1990**, *23*, 3339.
(11) Dalvi, M. C.; Eastmann, C. E.; Lodge, T. P. *Phys. Rev. Lett.* **1993**, *71*, 2591.
(12) Hoffmann A.; Sommer, J. U.; Blumen, A. *J. Chem. Phys.* **1997**, *107*, 7559.
(13) Chrissopoulou, K.; Rittig, F.; Fytas, G. In *Molecular Interactions and Time-Space Organization in Macromolecular Systems*; Morishima, Y., Norishima, Y., Tashiro, K., Eds.; Springer-Verlag: Berlin, 1999.
(14) Anastasiadis, S. H.; et al. *Europhys. Lett.* **2000**, *51*, 68.

MA0119068